

Supplementary information

Peptide epitope-imprinted polymer microarrays for selective protein recognition. Application for SARS-CoV-2 RBD protein

Zsófia Bognár ^a, Eszter Supala ^a, Aysu Yarman ^b, Xiaorong Zhang ^b, Frank F. Bier ^b, Frieder W. Scheller ^b and Róbert E. Gyurcsányi^{*a}

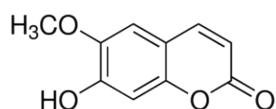
^a BME "Lendület" Chemical Nanosensors Research Group, Department of Inorganic and Analytical Chemistry, Budapest University of Technology and Economics, Szt. Gellért tér 4, 1111 Budapest, Hungary, E-mail: gyurcsanyi.robort@vbk.bme.hu

^b Institute of Biochemistry and Biology, University of Potsdam, Karl-Liebknecht-Str. 24-25, 14476 Potsdam OT Golm, Germany.

1. Experimental

1.1. Chemicals and reagents

GFNCYFP, GFNCYFPLQ and FNSYFPLQ peptides were custom-synthesized by Biosyntan GmbH (Berlin, Germany), negative control peptide (CGGGH) was synthesized by Bio Basic Inc. (Markham ON, Canada). The purity of all peptides was over 95%. The Recombinant 2019-nCoV Spike receptor binding domain (RBD) Protein with His tag, PBS, Tween 20, scopoletin (Scheme S1), (11-mercaptopoundecyl)tetra(ethylene glycol) (HS-TEG), human serum albumin (HSA) and potassium hexacyanoferrate(III) were purchased from Sigma-Aldrich. Absolute ethanol (AR grade) was ordered from Molar Chemicals Ltd. (Halásztelek, Hungary). Peptide stock solutions were prepared in Protein LoBind centrifuge tubes (Eppendorf) with RNase and DNase-free water for molecular biology (DEPC-treated and sterile filtered) (Sigma-Aldrich) containing 10% absolute ethanol. All aqueous solutions were made using deionized (DI) water of 18.2 MΩ cm resistivity at 25°C (Millipore Direct-Q 3 UV water purification system, Merck Millipore, Billerica, MA). Artificial saliva (ASTM E2720-16 and ASTM E2721-16 with 3 g/L mucin) was purchased from LCTech GmbH (1700-0316, Obertaufkirchen, Germany) and an extraction buffer of a commercially available Covid-19 saliva sample-based antigen test (Rapid Response[®] COVID-19 Antigen Test, BTNX Inc.) with 10 g/L protein content (determined by UV measurements at 280 nm) was used during the analysis. SARS-CoV-2 virus-like particles (VLP) were purchased from Abnova (P6677), and β-propiolactone-inactivated Influenza A (H3N2 subtype) virus particles were provided by Marc Eleveld and Professor Marien I. de Jonge (Radboud University, Nijmegen, The Netherlands).



Scheme S1. Structural formula of scopoletin.

1.2. Peptide microspotting onto gold SPRi chips

Gold SPRi chips purchased from Horiba (Palaiseau, France) were cleaned with piranha solution (1:3 of 30 % H₂O₂ and cc. H₂SO₄) for 20 minutes, rinsed with DI water and ethanol, followed by drying under Ar-stream. The SPRi chips were further cleaned, immediately before microspotting, in UV-generated ozone atmosphere (Novascan Technologies, Ames, IA, USA) for 30 minutes. For the imprinting, peptides were immobilized on the SPRi slides by microspotting using a BioOdyssey™ Calligrapher™ miniarrayer (BioRad, Hercules, CA, USA) with a 500 μm diameter SMP15 Stealth Micro Spotting Pin (Arrayit Corporation, San José, USA) having 0.25 μL uptake volume. The spottings were made from 20 μL peptide solutions of different concentrations in PBS, that were loaded in the wells of a Protein LoBind, PCR clean, 384 well LD-PE plate (Eppendorf). For the non-imprinted polymer (NIP) generation, PBS solutions (without peptides) were also microspotted. Three spots were made at each peptide concentration to assess on-chip reproducibility. The SPR image and layout of the spots of the epitope-imprinted polymer microarray, which was used for the investigation of spike protein RBD binding, is shown in Fig. 2/A. For SARS-CoV-2 VLP measurements, an extended microarray was used, where a spotting concentration of 2.5 μM of the GFNCYFP and GFNCYFPLQ peptides to prepare the epitope-imprinted polymer spots were also incorporated (Fig. S1).

For microspotting the relative humidity of the chamber was set to 65 rh% and the spotting stage was thermostated at 12°C. The spotted SPRi chips were incubated at 20±1°C and 65 rh% in the spotting chamber (to avoid the evaporation of the spotted microdroplets) for 2 h. The microspotted chips were gently dried under N₂ and stored at 4°C overnight. Before the deposition of the polyscopoletin film, i.e. insertion into the electrochemical cell, the chips were rinsed with DI water and dried under gentle N₂ stream.

Supplementary information

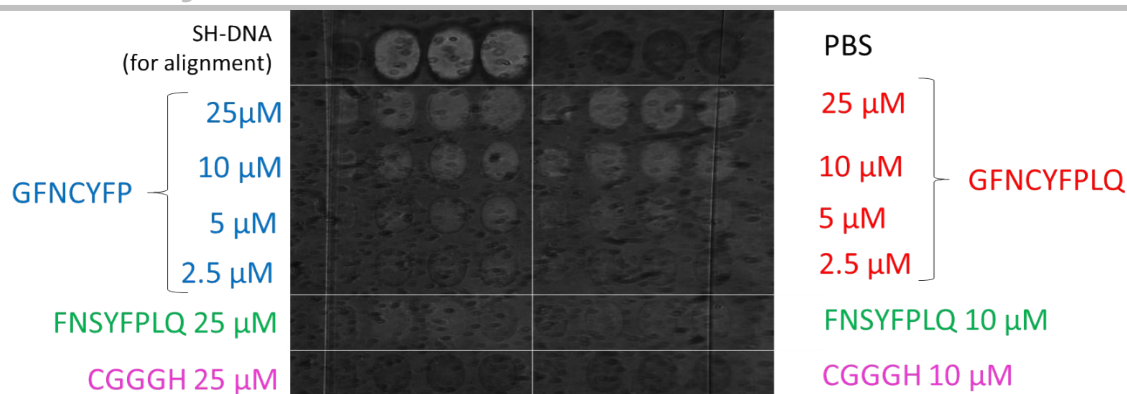


Fig. S1. SPR image and layout of the epitope-imprinted microarray used for SARS-CoV-2 VLP binding.

1.3. Electrochemical synthesis of the epitope-imprinted polyscopoletin film

The polyscopoletin film was deposited by electropolymerization onto the surface of gold chips microspotted with the different epitope and control peptides. The electropolymerization was performed using an Autolab PGSTAT12 potentiostat (Metrohm Autolab B.V., Utrecht, The Netherlands) in a three-electrode electrochemical cell in which the gold chip served as the working electrode a Ag/AgCl (3 M KCl) as the reference electrode and a Pt sheet as the counter electrode. The cell was filled with an aqueous solution containing 0.5 mM scopoletin, 5 V/V% ethanol and 0.1 M NaCl. The electropolymerization of scopoletin was carried out using 30 cycles of a potential step program in which 0.0 V was applied for 5 s and 0.7 V for 1 s. The polyscopoletin film deposition on the peptide spotted regions generated the respective epitope-imprinted polymer spots, while on the PBS spotted (or not-spotted) regions the non-imprinted polymer controls. The chips were then incubated for 1 h in a gently agitated solution of 0.5 mM HS-TEG solution in PBS, to block any exposed bare gold surface. Finally, the peptide epitope templates were removed by cleaving the Au-S bonds, i.e. by oxidative stripping in PBS applying 1.0 V for 20 s

1.4. SPRi measurements

The SPRi chips with the epitope-imprinted polymer microarray prepared on its surface were mounted on a glass prism using a high refractive index matching liquid. For the SPRi measurements a Horiba Plex II SPRi system (Horiba Jobin Yvon SAS, Palaiseau, France) was used at fixed optimal angle (selected based on the recorded angular scan curves). After insertion the surface of the chip was equilibrated for 90 minutes in PBST working buffer (PBS + 0.05% Tween20) at a flow rate of 50 $\mu\text{L min}^{-1}$. 180 μL of the different samples RBD, HSA, SARS-CoV-2 VLP and Influenza A (H3N2) formulated in PBST and Protein LoBind centrifuge tubes were injected into the SPRi flow cell and the binding was monitored in real time at 25.00 $^{\circ}\text{C}$, at a flow rate of 50 $\mu\text{L min}^{-1}$. The evaluation of the recorded SPR curves and calculation of the kinetic parameters was performed using Scrubber 2 (GenOptics version 2.0) software.

1.5. Atomic force microscopic (AFM) measurements

The polyscopoletin film thickness was measured with AFM (NanoSurf FlexAFM, Switzerland) using a Tap190AI-G cantilever (BudgetSensor, force constant: 48 N/m, length: 225 μm , tip radius < 10 nm). First, to obtain the topography of the polymer nanofilm, a 3 \times 3 μm area was scanned in Tapping mode (300 points/line resolution, 400 mV free amplitude, 88-90% set point). The polymer was then removed from a 1 \times 1 μm area in 3 consecutive cycles using Lateral Force mode with 200 points/line resolution and applying 1 μN force. Finally, the topographic image was recorded with the same parameters over a 3 \times 3 μm area, which included the polymer-stripped region. The images were analysed with Gwyddion software and the thickness of the polyscopoletin nanofilm was determined as the average difference between the polymer height and the liberated gold surface.

1.6. Determination of the size and concentration of SARS-CoV-2 VLP and inactivated Influenza A (H3N2) with nanoparticle tracking analysis (NTA)

NTA measurements were performed with a Nanosight LM10-HS system (Malvern Instruments Ltd.) using a 488 nm laser light source. The virus (SARS-CoV-2 VLP and Influenza A (H3N2)) particles were diluted in PBST to a nominal concentration of ca. 10^8 particles mL^{-1} and were injected with sterile syringe in the thin layer measurement cell of the NTA system at room temperature. The reported results are based on an average of 10 tracking records of 30 s and were calculated with the Nanosight NTA 2.3 software.

Supplementary information

2. Results and Discussion

2.1. Determination of the polyscopeletin nanofilm thickness by AFM

For the AFM measurements, an epitope-imprinted polymer microarray was prepared and the thickness of the nanofilm was determined as the average difference of the polymer height and the liberated gold surface (Fig. S2). According to the results obtained from 3 different locations, the surface was covered with a uniform polyscopeletin layer having a thickness of 10.2 ± 0.6 nm.

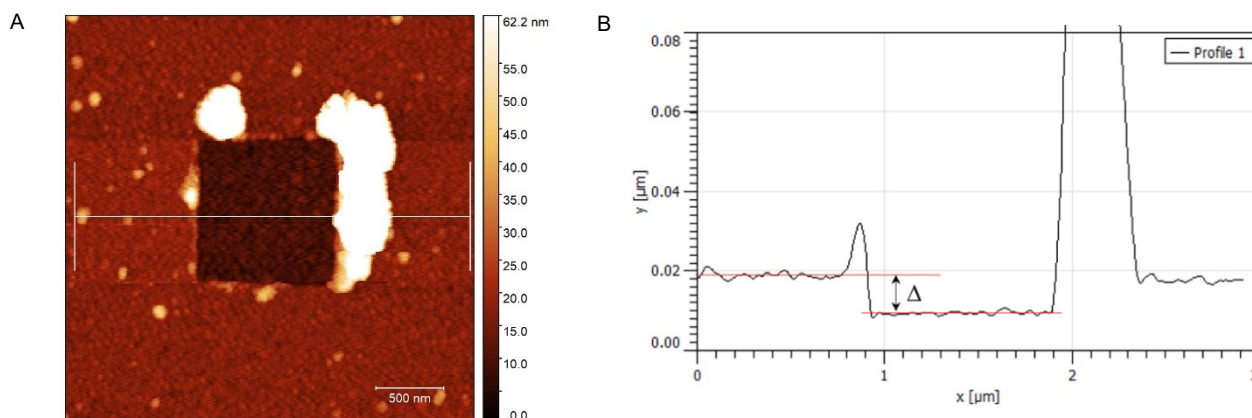


Fig. S2. The topographic image of the polyscopeletin nanofilm after removing the polymer from a 1×1 μm rectangular area as seen in the center of the image (A) and a representative cross-section profile (B) illustrating the film thickness (Δ) determination. The bright spots in (A) corresponding to larger heights are due to the removed polymeric material pushed to the side of the rectangular area during the removal process.

2.2. Stability of HS-TEG layer on gold during the electrochemical template removal program

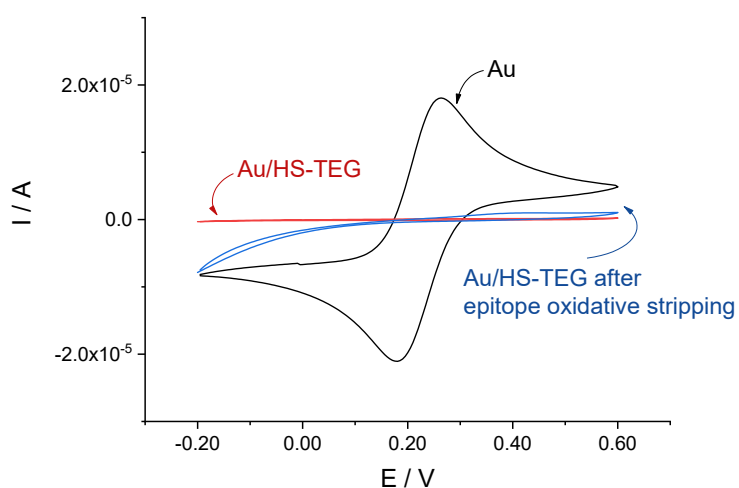


Figure S3. Cyclic voltammetry (CV) experiments in 5 mM $\text{K}_3[\text{Fe}(\text{CN})_6]$ (PBS) to confirm the stability of the HS-TEG on gold. Gold disk electrodes with 2 mm diameter (CH Instrument Inc.) were modified with 0.5 mM HS-TEG in PBS for 1 hour. After modification the surface confinement of HS-TEG was confirmed by the suppressed redox currents (Au/HS-TEG). The stability of the HS-TEG layer polarized at 1.0 V was confirmed by repeating the same CV experiment, which shows negligible current compared to the unmodified gold (Au). All CVs were performed in the range of $-0.2 - 0.6$ V at 50 mV/s with the 3rd cycle shown.

Supplementary information

2.3. SPR binding curves of RBD to epitope-imprinted MIPs

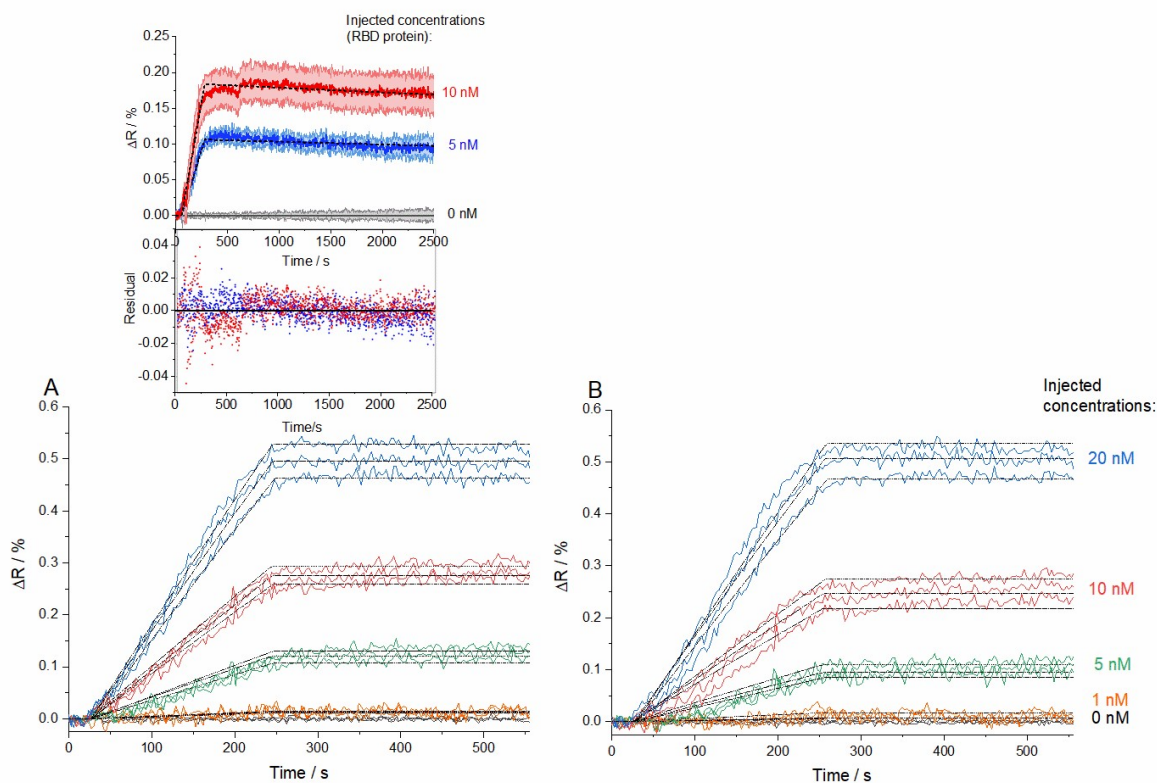


Fig. S4. SPR binding curves (sensorgrams) of RBD on GFNCYFP (A) and GFNCYFPLQ (B) peptide-imprinted polystyrene spots. The black, dashed lines are the theoretical fits of the experimental data. Different RBD concentrations (1-20 nM in PBST) are shown in different colors as indicated in the figure legend, i.e. the same color curves are indicative of the reproducibility of the epitope-imprinted polymer spots prepared in triplicates on the MIP microarray. The inset shows the prolonged dissociation time experiments.

2.4. Signal reproducibility of RBD binding across different MIP arrays

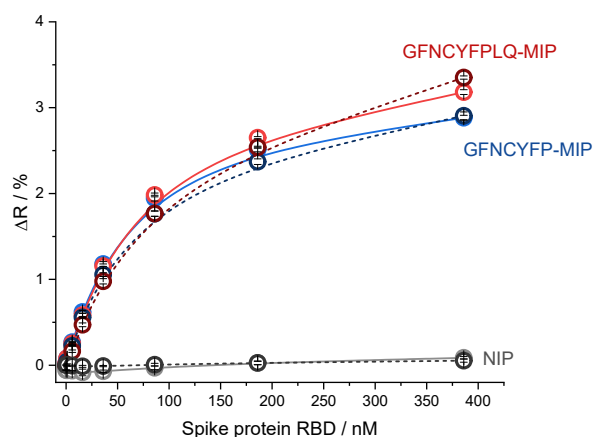


Fig. S5. SPRi signal reproducibility across different MIP chips. The solid and dashed curves show the binding of spike protein RBD on two different MIP-based SPRi chips prepared using the exactly same conditions (microspotting and electropolymerization). The figure compares measurements on GFNCYFP and GFNCYFPLQ epitope imprinted polystyrene spots (red and blue, respectively) and on NIP spots (black). The spotting solution concentration was 25 μ M for both peptides.

2.5. Investigation of the negative control FNSYFPLQ peptide adsorption on gold surface

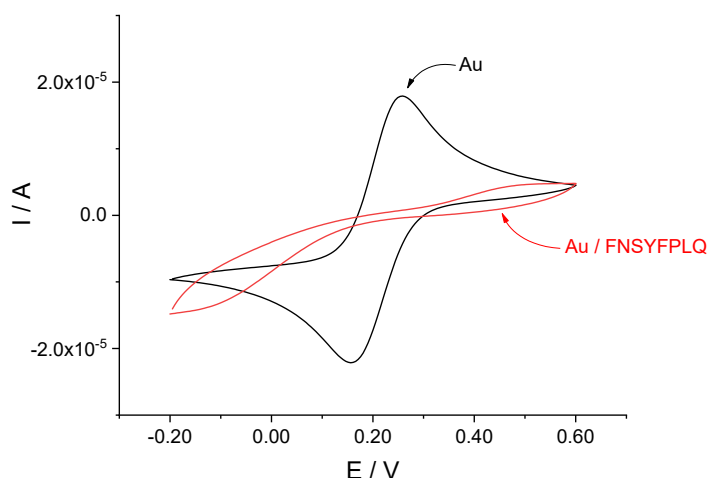


Fig. S6. Confirmation of the adsorption of negative control, FNSYFPLQ peptide on gold surface by cyclic voltammetry in 5 mM $K_3[Fe(CN)_6]$ (PBS). A gold disk electrode was incubated in 25 μ M solution of FNSYFPLQ peptide (in PBS) for 2 hours at 4°C and rinsed with DI water. The suppressed peak current (Au/FNSYFPLQ) as compared to the unmodified gold electrode (Au) confirm the adsorption of the peptide on the gold surface. The CVs were recorded in the range of -0.2 – 0.6 V at 50 mV/s. The 3rd cycle of the CVs are shown.

2.6. RBD binding of the epitope-imprinted microarray in complex sample matrices

The RBD binding to the various peptide-imprinted spots was investigated by kinetic titration in complex matrices, i.e. 100-fold diluted artificial saliva and commercially available Covid-19 antigen assay extraction buffer (Figure S6). The polymer spots imprinted with RBD stemming peptides (GFNCYFPLQ and GFNCYFP) showed selective recognition in both sample matrices while the RBD binding was negligible on the negative control peptide-imprinted polymers as well as NIP.

The sample matrix reduced the RBD binding-related signal in the artificial saliva and extraction buffer backgrounds with ca. 25% and 40%, respectively. The polymers imprinted with the longer peptide (GFNCYFPLQ) showed slightly higher binding capacity than with the shorter (GFNCYFP), which is in agreement with the results obtained in PBST (Figure 2.)

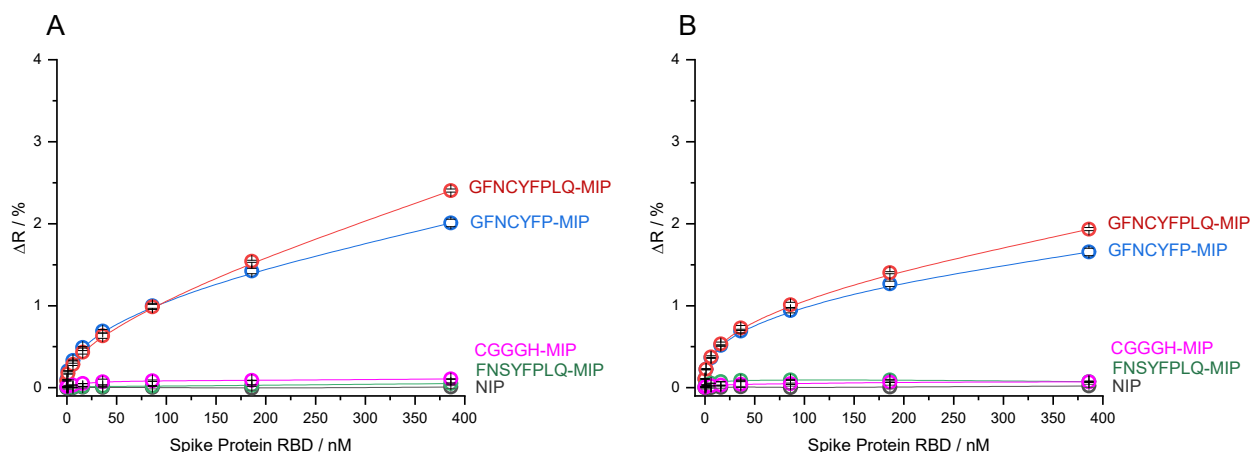


Fig. S7. Binding of RBD to peptide-imprinted polymer spots in 100-fold diluted artificial saliva (A) and extraction buffer (B).

2.7. Size and concentration determination of SARS-CoV-2 VLP and inactivated Influenza A (H3N2) virus

The size and concentration of the SARS-CoV-2 VLP and Influenza A (H3N2) virus was determined by nanoparticle tracking analysis, which is a single particle detection methodology that provide number-based distributions calculated directly from the set of individual particle sizes. The average particle diameter was ca. 80 nm for SARS-CoV-2 VLP (Fig. S8) and around 100 nm for Influenza A (H3N2) (not shown). The concentration of the particles was determined with NTA at five different concentration levels (inset) to confirm that no loss occurs during

Supplementary information

dilution. The concentration of the stock solution was $3.25 \cdot 10^{11} \pm 13.3 \cdot 10^9$ particles mL^{-1} for SARS-CoV-2 VLP and $4.22 \cdot 10^{11} \pm 2.67 \cdot 10^9$ particles mL^{-1} for Influenza A (H3N2).

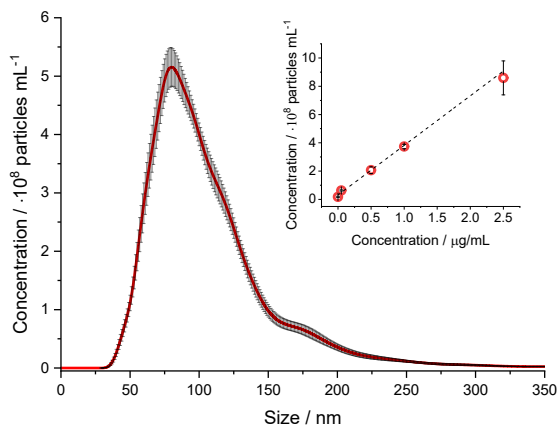


Fig. S8. Size distribution of SARS-CoV-2 VLP determined with NTA in PBST. For sizing 10 consecutive 30 s long measurements were performed. The concentration of VLPs was determined at five concentration levels to confirm the linearity of the dilution. The concentration of the stock solution was calculated as $3.25 \cdot 10^{11} \pm 13.3 \cdot 10^9$ particles mL^{-1} and the average diameter of the VLPs was ca. 80 nm.

2.8. AFM investigation of SARS-CoV-2 virus-liked particles bound to the MIP surface

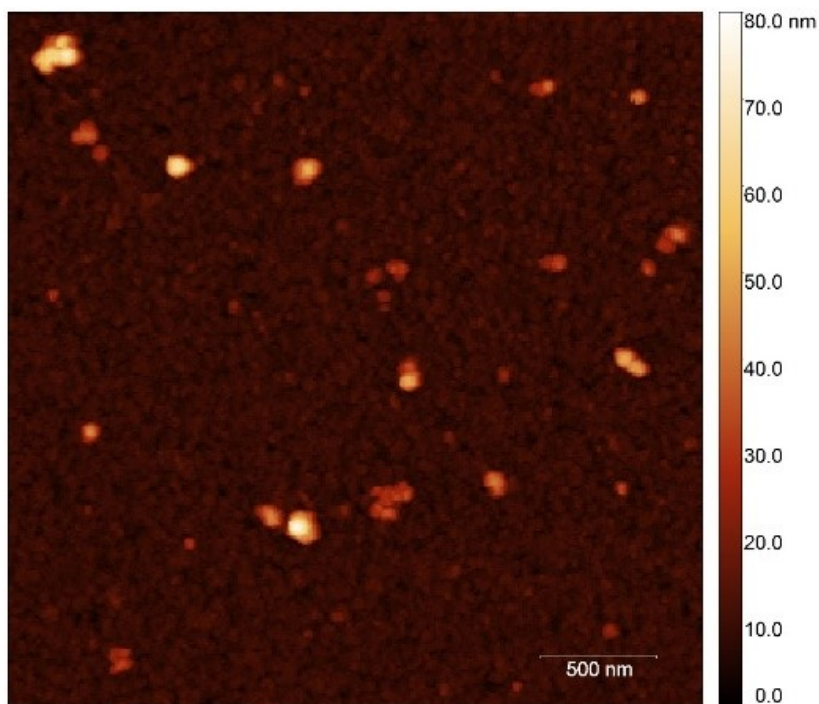
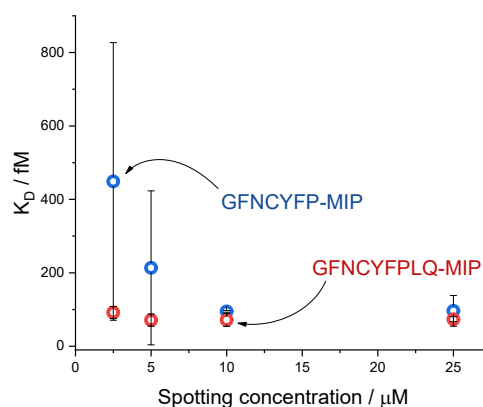


Fig. S9 AFM image of the SARS-CoV-2 VLP binding on the MIP surface. The AFM measurement were performed on a $3 \times 3 \mu\text{m}^2$ area of the epitope imprinted MIP in tapping mode after incubation with 1.1 pM VLP solution. The presence of the surface bound VLPs is clearly visible on the MIP surface in form of circular protuberances with a height and diameter of ca. 80 nm, which correlates well with the diameter of VLP obtained by NTA.

Supplementary information

2.9. The influence of the microspotted template epitope concentration on the affinity of the respective MIPs for



SARS-CoV-2 VLP

Fig. S10 Approximate K_D values of the interaction between hepta- and nonapeptide-imprinted polymer nanofilms and SARS-CoV-2 VLP as a function of the spotting concentration of the template peptides used for epitope imprinting. For the GFNCYFPLQ-imprinted polyscopoletin nanofilm, the K_D was ca. 100 fM independently of the template spotting concentration (surface concentration of the template). However, the shorter GFNCYFP-imprinted polyscopoletin nanofilms showed considerable increase both of the determined K_D values and their uncertainty as the template spotting concentration was lowered, but remained in the sub-picomolar range. Interestingly, the affinity of the MIPs prepared at different spotting concentrations of the nonapeptide GFNCYFPLQ was similar, however, for the heptapeptide-imprinted polymer spots, the K_D and its uncertainty significantly increased as the spotting concentration was lowered. **Of note the values reported despite of their consistency are rough estimates and apparent values given the limitation of the SPR technique to assess K_D values in the subpicomolar range. The error bars are result of the global fitting that does not account for other uncertainties!**